# Turbulent Particle Pinch in Tore Supra

G.T. Hoang, C. Bourdelle, X. Garbet, J.F. Artaud, V. Basiuk, J. Bucalossi, C. Fenzi-Bonizec, F. Clairet, C. Gil, R. Guirlet, F. Imbeaux, J. Lasalle, C. Lowry, B. Pégourié, B. Schunke, J.L.Segui, J. M. Travère, E. Tsitrone, L. Vermare
*Euratom-CEA Association, CEA/DSM/DRFC, CEA Cadarache*
*F-13108 Saint-Paul-Lez-Durance, France*

**Abstract** Steady state full non-inductive current Tore Supra plasmas offer an opportunity to study the local parametric dependence of particle pinch velocity, in order to discriminate among different theories. The existence of anomalous pinch is unambiguously demonstrated. The results support the turbulent theories based on Ion Temperature Gradient modes (ITG) and Trapped Electron Modes (TEM). In zero loop voltage plasmas, the density peaking is mainly determined by the profile of safety factor (q). An anomalous inward pinch generated by $\nabla q/q$ is found to be dominant in the gradient region (normalized radius $0.3 \leq r/a \leq 0.6$). In contrast, the direction of the anomalous pinch in the plasma core ($r/a \leq 0.3$) is more sensitive to the electron temperature ($T_e$) profile.

## 1 Introduction

Particle transport is being intensively investigated in most of current tokamak devices. It is one of crucial issues for magnetized fusion plasmas. Indeed, the density profile ($n_e$) plays an important role in the plasma performance. A peaked density profile can stabilize micro-instabilities (ITG and ETG) and reduce heat transport. In particular, it is favorable for fusion reactor, to enhance the fusion power ($P_{fus} \propto$ density) and to generate a large bootstrap current fraction ($\propto$ poloidal beta, thus density) required for continuous operation.

The general expression relating the particle flux ($\Gamma$) and the density ($n_e$) profile is:

$$\Gamma = - D.\nabla n_e + V.n_e \quad \text{(Eq.1)}$$

D is the diffusion coefficient and V is the sum of the neoclassical ($V_{neo}$) and anomalous ($V_{an}$) pinch velocities. $V_{neo}$ includes the so-called Ware pinch ($V_{Ware}$) [8] proportional to the toroidal electric field ($E_\varphi$), and the contributions of main ion temperature ($T_i$) and impurity density gradients. The existence of $V_{an}$ is predicted by turbulence theories based on ITG or TEM micro-instabilities. These theories predict two main mechanisms related to the profiles of the electron temperature [1,2] and of the safety factor [3,4], which are confirmed by several turbulence simulations and analytical approach [5-7]: i) turbulent thermodiffusion [1,2] generates a pinch velocity, inward or outward, proportional to $\nabla T_e/T_e$; ii) Turbulence Equi-Partition [3,4] drives an inward pinch proportional to $\nabla q/q$ (called curvature pinch). Accordingly, Eq.1 can be expressed as:

$$\Gamma = -D\,[\nabla n_e + (C_q\,\nabla q/q - C_T\,\nabla T_e/T_e)\,n_e] + V_{neo}\,n_e \quad \text{(Eq.2)}$$

Anomalous particle pinch has been invoked in several experiments: DIII-D [9], JET [10], TCV [11], TEXT [12], TFTR [13]. But in several cases, a neoclassical pinch is high enough to explain the peaked electron density profile (e.g., AUG [14], JET [15]). These experiments, in fact, have been carried out in conditions where either the resistive current does not vanish, thus $E_\varphi$ still subsists, or without an ignorable central particle source (i.e., using neutral beam heating). Therefore, the respective contribution of the neoclassical and anomalous pinches to the density profile peaking cannot be clearly identified. Recently, significant experimental and computational results are recorded. Evident of anomalous pinch has been observed in experiments with Electron Cyclotron Current Drive (ECCD, e.g., in TCV experiments [16]) or Lower Hybrid Current Drive (LHCD, in Tore Supra experiments [17]).

In Tore Supra experiments, the anomalous pinch has been unambiguously identified. Peaked $n_e$ profile has been maintained over a time ~80 times longer than the current diffusion time. Taking advantage of these plasma conditions, the local parametric dependence of anomalous pinch is investigated in order to discriminate among thermodiffusion and Equi-Partition

mechanisms. The main finding of the present work is that the thermodiffusion is found to be small. The density profile is mainly governed by an inward pinch driven by $\nabla q/q$ in the gradient region (normalized radius $0.3 \leq r/a \leq 0.6$, a being the plasma minor radius). Nevertheless, the direction of the pinch in the plasma core ($r/a \leq 0.3$) is rather sensitive to $\nabla T_e/T_e$ [18] when the Ware pinch vanishes.

## 2 Evident anomalous pinch

Very long discharges can be routinely obtained in Tore Supra, at zero loop voltage, thanks to full real time control implemented recently [19, 20]. Sawtooth free LHCD discharges, with duration up to 6 minutes, were performed at: plasma current $I_p = 0.5 - 0.7$ MA, central density $n_e(0) = 2 - 3.5$ x$10^{19}$m$^{-3}$, central electron temperature $T_e(0)$ up to 8 keV, central ion temperature $T_i(0) \leq 2.5$ keV, effective charge $Z_{eff}$ around 2. These plasmas were well diagnosed. Electron density and temperature profiles are measured by various diagnostics such as interferometry, Thomson scattering and a superheterodyne radiometer. In particular, the density profile is accurately measured by a powerful reflectometry system with high temporal resolution ($\Delta t$ = 25 µs) [21]. In addition, the current density profile was reconstructed by the integrated package of codes CRONOS [22] using the profile of fast electron bremsstrahlung to determine the LHCD current profile. Fast electron profiles are measured by a Hard-X ray tomographic system [23]. It is moreover constrained by the measurements of Faraday rotation angles and of plasma inductance. Interpretative analyses are performed in a fully self-consistent manner: the whole system of transport equations together with the current diffusion, the plasma equilibrium and the sources (i.e. heat and non-inductive current) for multiple species plasmas are computed by CRONOS. They provide therefore confidently the profile of $E_\varphi$, thus the neoclassical pinch computed with the code NCLASS [24] of the package CRONOS. In these plasmas, the plasma current was fully driven by LHCD over a time much longer than the current diffusion time. Transformer flux was kept exactly constant using the real time controls. $E_\varphi$ vanished thoughout the plasma cross section after a few tens of seconds, thus the Ware pinch. In these unique conditions, the density profile is found to be significantly peaked, with negligible central particle source. As shown in Fig.1, the value of the density peaking (defined as $n_e(0)/\langle n_e \rangle$ where $\langle n_e \rangle$ is the volume averaged value) is arround 1.6 when vanishing $E_\varphi$ measured at the last closed surface. Time evolution of a plasma lasting 6 minutes, with real time zero loop voltage control, is illustrated in Fig. 2. It can be seen that the density profile is peaked ($n_e(0)/\langle n_e \rangle \sim 1.6$) while $E_\varphi$ is null over 6 min. In this case, there is no central fuelling since the plasma was heated by the LH waves. The same density peaking was observed in both deuterium and helium plasmas. Main particle sources from the external gas puffing and the recycling on the pump limiter have been evaluated with the 3D neutral code EIRENE [25] and are found to be located in the outer part of the plasma. As shown in Fig. 3a, the radial profile of these sources indicates that less than 1% of total ionized deuterium, is located inside r/a = 0.7. This result is consistent with $n_e$ profiles measured by

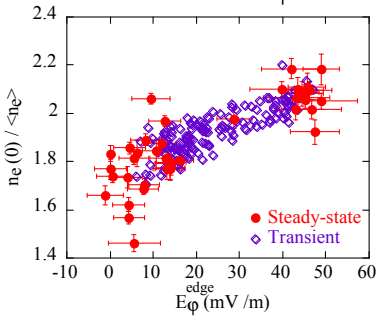


*Fig.1: Variation of density peaking as function of inductive toroidal electric field measured at the last closed surface during both transient and steady-state phases for a series of 30 discharges*

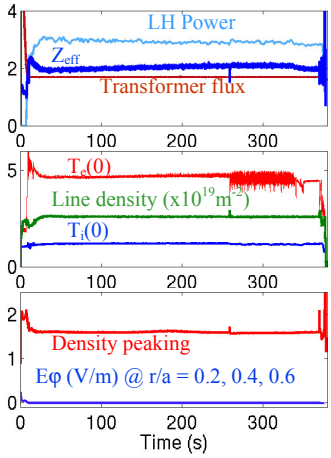


*Fig. 2: Time evolution of a full LHCD plasmas (#33299).*

reflectometry (Fig. 3.b), which exhibit a gradient in the edge region higher. The ionisation source due to the intrinsic impurities, mainly Carbon and Oxygen, was also evaluated. Its contribution to the electron density was evaluated consistently with the measurements of $Z_{eff}$, $T_i$ and the neutron rate, taking into account $C^{6+}$ and $O^{8+}$ ionization stages. The fraction of electrons due to these ion impurities ( ~ $3x10^{18}m^{-3}$) is small compared with $n_e \geq 1.5\ x10^{19}m^{-3}$ inside r/a = 0.7. Therefore, the peaked $n_e$ profile inside the core region ($r/a \leq 0.6$) is related to the particle transport properties, not to the central source. The observed inward pinch has to be anomalous. Since $V_{neo}$, mainly due to the impurity contribution, does not exceed the value of $1x10^{-3}$ m/s.

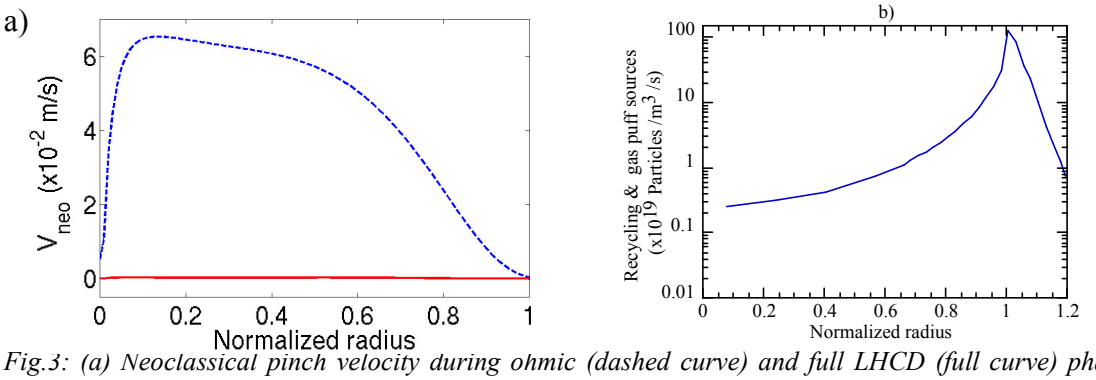


*Fig.3: (a) Neoclassical pinch velocity during ohmic (dashed curve) and full LHCD (full curve) phases of the discharge displayed in Fig. 2, respectively at t = 4s and 140 s; (b): Ionization source from the external gas puffing and recycling, computed with the 3D EIRENE code.*

Inside r/a =0.6, the ratio $V_{an}/D$ is determined by the measured $n_e$ profile: $V_{an}/D = \nabla n_e/n_e$ (see Eq. 2). Its radial profile is shown in Fig. 4. It can be seen that $V_{an}/D$ is close to 1 $m^{-1}$ in the region r/a = 0.2 - 0.7. To evaluate $V_{an}$, a 1D simulation has been performed with a model described in Ref [26] taking into account the parallel particle sink in the scrape off layer. In the present case, D is assumed to be the same as in the ohmic phase [27] (under estimated since we do not take into account the power degardation of the confinement).

*Figure. 4: Radial profile of the ratio $V_{an}/D$, deduced from $n_e$ profile*

The simulation well reproduces the measured $n_e$ profile (Fig. 5a). To obtain the right simulated profile, we need a value of $V_{an}$ two orders of magnitude higher than $V_{neo}$ in the gradient region, and up to 10 m/s at the plasma periphery, as shown in Fig. 5b. Of course, one could simulate the same $n_e$ profile by imposing a pinch velocity of the order of neoclassical (<$10^{-3}$ m/s) and D unrealistically lower than the collisional value ~ $2x10^{-3}$ $m^2/s$.

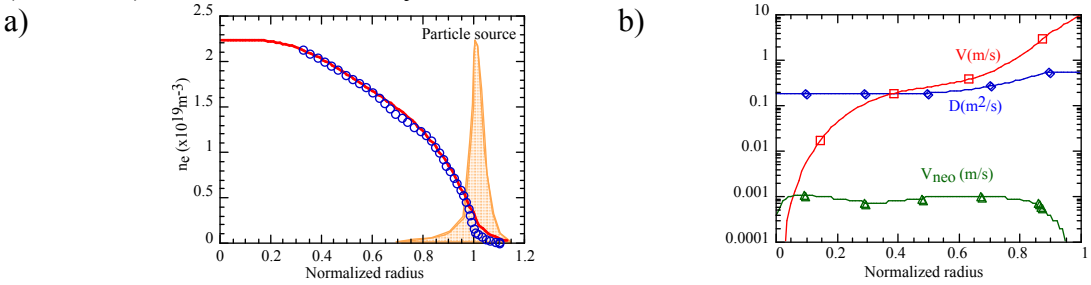


*Fig. 5: 1D simulation of $n_e$ profile measured by reflectometry. a), Experimental (circles) and simulated (full line) $n_e$ profile. b), Corresponding $V_{an}$ (full line/squares, in m/s) and D (full line/diamonds, in $m^2/s$). $V_{neo}$ is computed by NCLASS (full line/triangles).*

It is worth noting that the LH waves could contribute to this anomalous pinch due to: i) the electric field of the waves; ii) the detrapping of fast electrons. So far, such a contribution cannot be confidently provided by existing codes. However, careful analysis of the time evolution of $\nabla n_e/n_e$ indicates that the part due to the first mechanism cannot exceed $V_{neo}$ (see

for example Fig. 7b in §3.1, where $\nabla n_e/n_e$ is seen to decrease when vanishing $V_{neo}$ without any correlation with the LH power which is rised up). For the second mechanism, the suprathermal electrons cannot be detrapped by collisions since their energy is between 75 keV and 175 keV. The main loss is due to the ripple which is < 5% in Tore Supra. To maintain the observed $n_e$ peaking through this mechanism, an unrealistic pinch velocity of ~100 km/s is needed, taking into account a measured suprathermal density which is less than 0.1% of the thermal population [28]. In consequence, the pinch driven by the LH waves can be ruled out in our experiments.

## 3. Parametric dependence of anomalous pinch

Turbulent simulations have been intensively performed to quantify two turbulent pinches in Eq.2 [5-7]. But experimentally, It is quite impossible to identify different effects in Eq. 2 when the plasma is inductive because of the complex interplay between $T_e$, q and $E_\varphi$ profiles through the plasma resistive current. In several experiments, the density peaking is found to be related to either $T_e$ (AUG [29]) or the q-profile (JET [30], DIII-D [12], TCV [16], TFTR [3]).

Taking advantage of full LHCD discharges described in Sec. 2, we have studied the dependences of $V_{an}$ on $\nabla T_e/T_e$ and on $\nabla q/q$. According to Eq.2, inside r/a = 0.6, since source and $V_{neo}$ are negligible, the density peaking is determined, by:

$$\nabla n_e/n_e = - C_q \nabla q/q + C_T \nabla T_e/T_e \qquad \text{(Eq. 3)}$$

To separate the effects of these two parameters, we vary one of them in fixing the other constant. For this purpose, we have selected a set of seven full LHCD plasmas without sawteeth. Because of the well known stiffness of $T_e$ profile [31,32], $\nabla T_e/T_e$ cannot be varied substantially at a given radial position in keeping $\nabla q/q$ constant. The main parameters in the data set are the following: $n_e(0) = 2.2\text{-}3.5 \times 10^{19} m^{-3}$, $q_{edge}$ = 9-14, q(0) = 1.2-2, $T_e(0)$ = 4.5-7.8 keV, $T_i(0)$ = 1.5-2.5 keV. For each discharge, the radial profiles are taken over time intervals of 1 s or 2 s.

### 3.1 $\nabla T_e/T_e$ dependence

Variation of $\nabla n_e/n_e$ versus $\nabla T_e/T_e$, at fixed $\nabla q/q$ value, is shown in Fig. 6. The slope and origin of the linear fit correpond respectively to $C_T$ and $C_q$ (Eq. 3). The result clearly indicates the thermodiffusion pinch has two opposite directions belonging two regions. Its direction is found to change from outward ($C_T < 0$) to inward ($C_T > 0$) when moving from the outer to the inner plasma. This behavior seems to be correlated with increasing the ratio $\nabla T_e/\nabla T_i$ (from 0.7 to 4.8), as expected in 3D non-linear turbulence simulations in Ref. [6]. We first examine the core region r/a ≤ 0.3. As shown in Fig. 6a, $\nabla n_e/n_e$ linearly increases when increasing $\nabla T_e/T_e$. Best fits indicate that both thermodiffusion and curvature pinches are small. Within the error bar, the thermodiffusion pinch seems to be slightly larger than the curvature pinch: $C_T \sim 0.2$ and $C_q \sim -0.1$. Note that the sign of $C_q$, thus the direction of curvature pinch is not accurately determined.

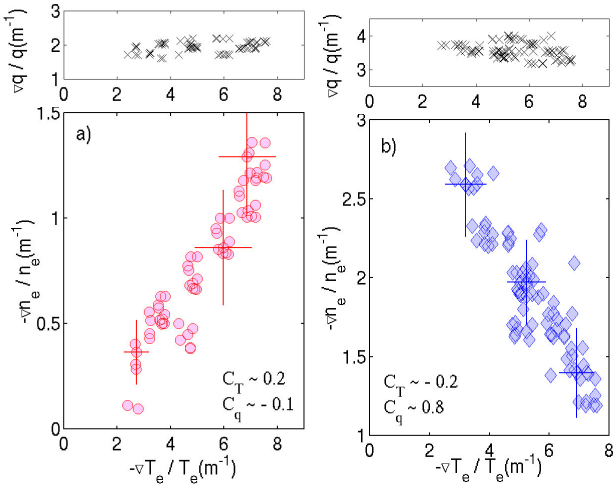


*Fig. 6: $\nabla n_e/n_e$ versus $\nabla T_e/T_e$ with corresponding $\nabla q/q$ (cross), from a set of seven discharges. (a) r/a ≤ 0.30, $T_e/T_i$ = 2 ± 0.4, $\nabla T_e/\nabla T_i$ = 3.8 – 4.8. (b) 0.35 ≤ r/a ≤ 0.6, $T_e/T_i$ = 1.2 ± 0.4, $\nabla T_e/\nabla T_i$ = 0.7 – 3.5.*

In contrast, in the gradient region, $0.35 \leq r/a \leq 0.6$, the outward thermodiffusion flux is dominated by the inward curvature flux. As shown in Fig. 6b, linear fit of $\nabla n_e/n_e$ versus $\nabla T_e/T_e$ give $C_T \sim -0.2$ which is smaller than $C_q \sim 0.8$. Thus, it seems to be dificult to isolate this thermodiffusion contribution.

In the plasma core ($r/a < 0.3$), the inward thermodiffusion cannot be clearly identified when the inductive current is not completely relaxed. In this situation, the subsisting $V_{Ware}$ dominates. An example in shown in Fig. 7 which displays a discharge lasting 2 minutes with combined LHCD and Ion Cyclotron Resonance heating (ICRH). During the relaxation of the current (from 6s to 12s), after the LH power application, the flattening of $n_e$ profile in a narrow plasma core is due to the decrease of $V_{Ware}$, not to the change in $T_e$ profile.

As shown in Fig. 7b, the value of $\nabla n_e/n_e$ at $r/a = 0.3$ decreases by a factor of about 2 when the Ware pinch drops to zero due to the decrease of $E_\varphi$, while the value of $\nabla T_e/T_e$ swings between 2 and 4. A weak effect of the thermodiffusion can only be identified in the plasma core region when the Ware pinch is completely suppressed. It can be seen in Fig. 7c, an increase of $\nabla n_e/n_e$ of roughly 30% is clearly correlated with the increase of $\nabla T_e/T_e$ from 2 to 4 (consistent with a weak change seen in Fig. 6a), while $V_{neo}$ is negligible corresponding to the absence of $V_{Ware}$ over 20 s. Here, $V_{neo}$ is computed with the code NCLASS taking into account all neoclassical effects, including the pinch driven by the temperature and density gradients of all particle species. During this phase, weak variations of $\nabla q/q$ (~20%) within the error bars cannot be responsible for the change of $\nabla n_e/n_e$.

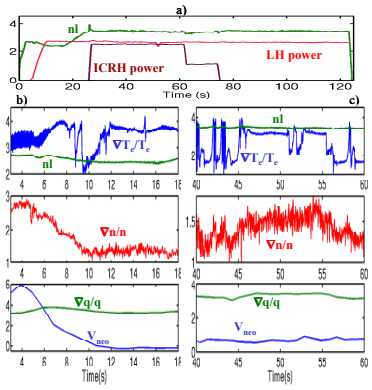


*Figure 7: Combined ICRH and LHCD discharge: (a) central line density (nl in $10^{19}m^{-2}$), LH and ICRH power in MW; (b) Correlation between $\nabla n_e/n_e$ and the Ware pinch at $r/a = 0.3$; (c) Correlation between $\nabla n_e/n_e$ and $\nabla T_e/T_e$ (in $m^{-1}$), at $r/a = 0.3$, when vanishing Ware pinch ($V_{neo}$ in $10^{-2}$m/s including all neoclassical effects).*

### 3.2 ∇q/q dependence

The dependence on $\nabla q/q$ has been studied in the gradient region ($0.3 \leq r/a \leq 0.6$), with $\nabla T_e/T_e = 6 \pm 0.6$, selected from the data set. In this region, we found, again, an inward curvature pinch which dominates outward thermodiffusion pinch . As shown in Fig. 8, $\nabla n_e/n_e$ increases linearly as a function of $\nabla q/q$ with a positive slope: $C_q \approx 0.8$ and $C_T \approx -0.15$. This result is in agreement with the observations in JET L mode [30] and TCV [33] which exhibited a correlation between the density peaking and the plasma inductance relating to global magnetic shear.

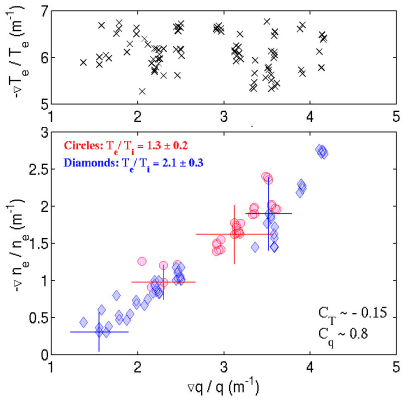


*Fig. 7: $\nabla n_e/n_e$ versus $\nabla q/q$ within $0.3 \leq r/a \leq 0.6$ from a set of seven discharges, keeping $|\nabla T_e/T_e|$ at the value of $6 \pm 0.6$ $m^{-1}$ (cross) and $\nabla T_e/\nabla T_i = 0.6 \pm 0.3$*

Micro-stability analysis of these discharges has been analyzed using the linear electrostatic gyro-kinetic code KINEZERO [34]. The spectra of linear growth rate ($\gamma$) of the unstable electrostatic eigenmodes have been calculated taking into account the non adiabatic response of both ion and electron populations, covering large ($k_\theta \rho_i < 1$, corresponding to ITG and TEM) and small scales ($k_\theta \rho_i > 1$, corresponding to TEM and ETG) instabilities. In these discharges, the electron-ion collision frequency $\nu_{ei}$ is between $0.5 \times 10^4$ $s^{-1}$ and $4 \times 10^4 s^{-1}$ for $0.1 \leq r/a \leq 0.6$,

to be compared to the vertical drift frequency of trapped electrons $\omega_{De} = 0.5x10^5$ - $1x10^5 s^{-1}$ at $k_\theta \rho_i = 1$. The corresponding effective collision frequency $\nu_{eff} = (5/2)^{1/2} \nu_{ei} R/c_s$, as defined in [35], is between 0.1 and 0.3. Thus, the trapped electron contribution is not negligible [36]. To quantify this contribution, we have performed two KINEZERO calculations. In the first one, the effect of collisions is neglected ($\nu_{eff} = 0$). In the second case, we neglect the trapped electron contribution ($\nu_{eff} >> 1$).

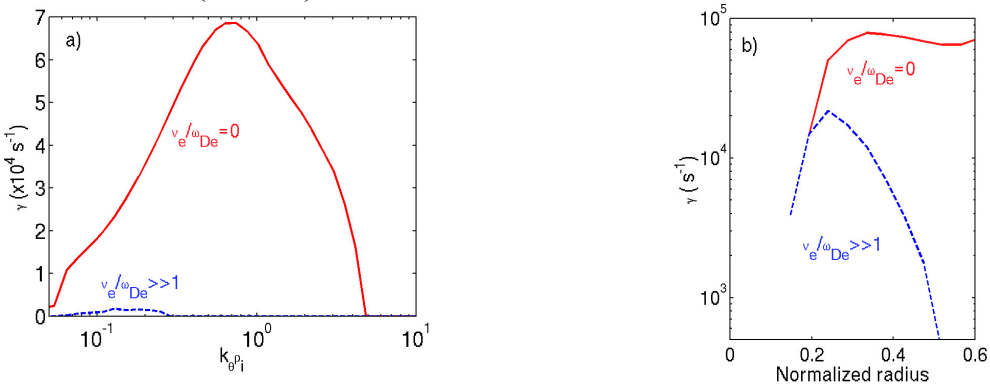


*Fig. 8: Micro-stability analysis of a full LHCD discharge: (a) Spectrum of linear growth rate at mi-radius; (b) Radial profile of maximum growth rate. Full curves: $\nu_e/\omega_{De}=0$ (mixed ITG and TEM); dashes curves: $\nu_e/\omega_{De}>>1$ (absence of TEMs).*

The results of the analyses indicate that ITGs and TEMs are destabilized inside the region r/a ≤ 0.6. While the ETG modes are found to be stable at all radii. TEMs are more and more dominant when moving from the core to the gradient zone. Conversely, in the core r/a < 0.3, the unstable modes are purely ITG. The complete spectra of γ calculated at mid-radius and radial profiles of maximum growth rate are shown respectively in Fig. 9a. and in Fig. 9b. Correlation between TEM unstable modes and dominant inward curvature pinch, in the gradient region, is in agreement with previous results of transport simulations [6, 7, 36] in the $n_e$ profile, are shown in Fig. 10. In this figure, both the measured and predicted profiles of $n_e$ are normalized to the value at r/a = 0.6. As can be seen in Fig. 10a, the empirical model proposed by Boucher *et al.* in Ref [37], $n_e \sim 1/q^{0.5}$, matches well the experiments. This model has been tested, previously in Ref [37], as against JET L/H-mode discharges and the ITER database. When using the prediction $n_e \sim 1/q$, as proposed by Nycander and Yankov [38], we over estimate the density peaking (Fig. 10b). The formula based on ITGs as proposed by Isichenko *et al.* [3] $\frac{n(r)}{n(0)} = 1 - \frac{1}{R}\int_0^r (\frac{1}{2} + \frac{4}{3}s)$, is found to be in agreement with experiments. It somewhat underestimates the $n_e$ peaking for low q discharges.

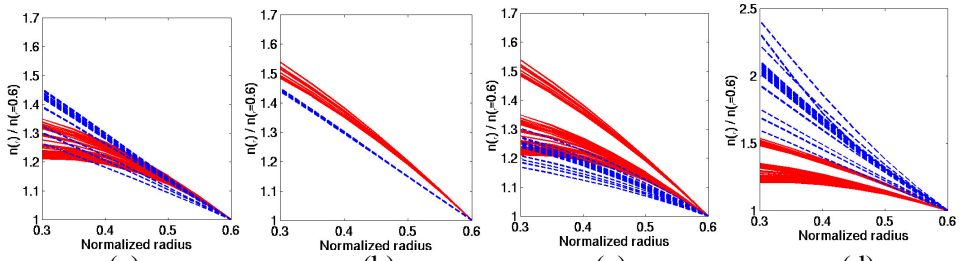


*Fig. 10: Comparison of measured $n_e$ profiles (full) with prediction (dashed). (a) ; Boucher&Rebut ($n_e \sim 1/q^{0.5}$)low q discharges; (b) Boucher&Rebut, high q discharges; (c), Isichenko et al. ; (d) Nycander &Yankov (1/q).*

## 4. ITER performance taking into account turbulence pinch

Anomalous curvature pinch, leading to a peaked density profile, could have beneficial effects on micro-instability stabiliation and on reduction of heat transport. Since $n_e$ peaking depends on the q-profile. There is therefore a possiblity to control ITG/ETG instabilities through the

q-profile control using an external non-inductive current drive method (for example ECCD or LHCD). Moreover, peaked density profile enhances the fusion power. Stability analysis of standard ITER plasma target, performed with the code KINEZERO, indicates that TEMs are expected to be present. In such a plasma, $\nu_{eff} = 0.1\text{-}0.2$ is similar to the Tore Supra conditions. Therefore, curvature pinch will potentially exist in ITER plasmas. Its impact on the performance of ITER has to be investigated.

For this purpose, we have performed a tentative simulation of the ITER reference scenario with 40MW of Neutral Beam Heating as defined in Ref [39], using the 0D module of the integrated code CRONOS. This simulation has been performed in a consistent manner using various empirical scalings, namely boostrap current [40] and $Z_{eff}$ [41]. In particular, we used the conservative scaling ITERH-98P(y,2) [42] less favorable in beta dependence for global energy confinement. In this simulation, the density peaking is assumed to be consistent with $n_e \sim q^{-0.5}$, according to the results in Ref [37] and in Tore Supra. Plasma dilution due to an eventual impurity accumulation is not taken into account. But it includes an increase of $Z_{eff}$ which varies from 1.55 to 1.7 due to its dependence on the radiated power that increases itself with $n_e$. The results of simulations show a potential gain of about 30% on ITER performance when including the effect of curvature pinch.

As shown in Fig. 11, the fusion power is around 530 MW corresponding to a fusion gain Q~13 (defined as the ratio of the fusion power and the input power), to be compared with $P_{fus}$ = 390 MW (Q=10) when using a flat density profile assumed in ITER. Note that, for the flat $n_e$ case, our 0D code provides - in spite of its simplicity (one simulation requires 3 min of CPU) - the expected value of $P_{fus}$ (400 MW) obtained with much more complex codes, within the error bar of 2.5%.

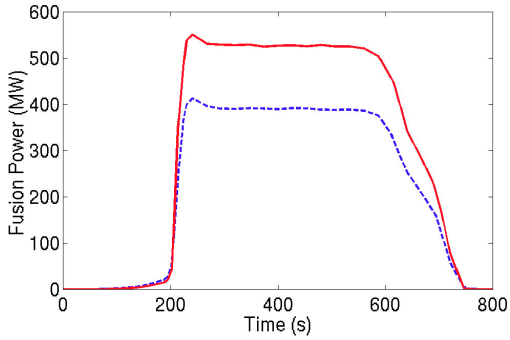


*Fig. 11: Fusion power expected in ITER reference scenario(with 40MW of NBI). Dash: using ITER assumed flat $n_e$. Full: with $\nabla n_e/n_e = 0.5\ \nabla q/q$*

When using a more favorable global confinement scaling without beta dependence, recently proposed in Ref [43], a larger amount of fusion power is expected for ITER. However, the gain due to the density peaking is smaller, about 22%. A fusion power of 1.1 GW is obtained taking into account the curvature pinch, compared to 900 MW in the flat profile case.

## 5. Conclusions

Turbulent particle pinch is now evidently observed in tokamaks. In Tore Supra, it is responsible for peaked density profiles in steady-state conditions. Peaked density profiles were maintained over 6 minutes in discharges fully driven by LHCD by a particle pinch velocity two orders of magnitude above the neoclassical value.

The results of parametric dependence study support the turbulent transport theories based on ITGs and TEMs. The main findings are that both the thermodiffusion and magnetic curvature pinches co-exist. Thermodiffusion pinch is found to be small. Its direction changes from outward to inward when moving from the plasma outer part to the center, correlated with respectively dominant TEM and ITG modes.

In the gradient region (r/a = 0.3-0.6), the pinch driven by $\nabla T_e/T_e$ is outward, but its effect on the density profile is weak. The electron density profile is mainly determined by an inward pinch generated by $\nabla q/q$, correlated with TEM dominant unstable modes. In contrast, $n_e$ profile peaking in the plasma core ($r/a \leq 0.3$) is more sensitive to the temperature gradient driven inward pinch, correlated with dominant unstable ITG branch, that can only be

observed when the Ware pinch is completely supressed. The change of the direction of thermodiffusion flux with the nature of micro-turbulence is predicted in Ref [6].
In order to give additional support to the present results, the measurements of fluctuations are being investigated in Tore Supra with a significant improvement of the reflectometry system [21].
Finally, the impact of turbulent pinch on ITER performance has to be investigated for predictive simulations, since TEM and ITG modes should be present in ITER plasmas.


[1] B. Coppi and C. Spight, Phys. Rev. Lett. **41** (1978) 551
[2] W.Tang *et al*., Phys. Fluids **29** (1986) 3715
[3] M.B. Isichenko, A.V. Gruzinov, P.H. Diamond, Phys. Rev. Lett. **74** (1996) 4436
[4] D.R. Baker and M.N. Rosenbluth, Phys. Plasmas **5** (1998) 2936
[5] F. Miskane, *et al.*, Phys. Plasmas **7** (2000) 4197
[6] X. Garbet, *et al*., Phys. Rev. Lett. **91** (2003) 035001
[7] C. Angioni, *et al*., Phys. Plasmas **10** (2003) 3225
[8] A. A. Ware, Phys. Rev. Lett. **25** (1974) 916
[9] Baker, *et al.*, Nucl. Fusion **40** (2000) 1003
[10] L. Garzotti, *et al.*, Proc. 29th EPS Conf., Montreux, Vol. 26B, P1.035 (2002)
[11] H. Weisen and E. Minardi, Europhys. Lett. **56** (2001) 542
[12] K.W. Gentile *et al*., Plasma Phys. Control. Fus. **29** (1987) 1077
[13] R.J. Hawryluk et al., Phys. Rev. Lett. **66** (2003) 421
[14] J. Stober, *et al.*, Nucl. Fusion **41** (2001) 1535
[15] M. Valovic, *et al*., Plasma Phys. Control. Fusion **44** (2002) 1911
[16] Zabolotsky *et al*., Plasma Phys. Control. Fusion **45** (2003) 735
[17] G.T. Hoang, *et al*., Phys. Rev. Lett. **90** (2003) 155002
[18] G.T. Hoang *et al*., Phys. Rev. Lett. **93** (2004) 135003
[19] D. van Houtte *et al*., Nucl. Fusion **44** (2004) L11-L12
[20] J. Jacquinot *et al.*, these proceedings
[21] R. Sabot *et al*., these proceedings
[22] V. Basiuk *et al*., Nucl. Fusion **43** (2003) 822
[23] Y. Peysson and F. Imbeaux, Rev. Sci. Instrum., **70** (1999) 3987
[24] W. A. Houlberg *et al.*, Phys. Plasma **4** (1997) 3230
[25] D. Reiter, Technical report Jül-2599 KFA-Jülich, 1992, http://www.eirene.de/
[26] B. Pégourié *et al*., Journal of Nucl. Mat., Vol.313-316 (2003) 539
[27] P. Laporte *et al.*, Proc. 21st EPS Conf., Montpellier, Part I (1994) 63
[28] J.L. Segui, G. Giruzzi, Proc. of in Diagnostics for Contemporary Fusion Experiments Workshop Varenna (1991), Editrice Compositori, Bologna (1992) 795.
[30] H. Weisen *et al*., Plasma Phys. Control. Fusion **46** (2004) 751
[31] F. Ryter, el al., Phys. Rev. Lett **86** (2001) 2325
[32] G.T. Hoang *el al*., Phys. Rev. Lett **87** (2001) 125001
[33] H. Weisen et al, *Nuclear Fusion* **42** (2002) 136
[34] C. Bourdelle *et al*., Nucl. Fusion **42** (2002) 892
[35] X. Garbet et al., Proc. 31st EPS Conf. on Controll. Fus. and Plas Phys. (2004)
Plasma Phys. Control. Fusion, issue dec 2004
[36] C. Angioni *et al*., Phys. Rev. Lett. **90** (2003) 205003
[37] D. Boucher, P.H. Rebut, Academie Sciences. T315, Ser. II, 273 (1992)
[38] J. Nycander and V. V. Yankov, Phys. Plasmas **2** (1995) 2874
[39] ITER, http://www.iter.org/
[40] G.T. Hoang *et al*., Proc. 24th EPS Conf. on Controll. Fus. and Plas. Phys., 21A Part III (1997) 965.
[41] G. F. Matthews, J. Nucl. Mater. 241-243 (1997) 618
[42] ITER Physics Basis, Nucl. Fusion **39** (1999) 2208
[43] D.C. McDonald *et al*., Plasma Phys. Contr. Fus. **46** (2004) A215